Analyses and Applications of Nonlinear Liquid Systems on Vibration Isolation

Wenlung Li[1], YuYen Wei[2]
[1]Professor, [2]Graduate Student
National Taipei University of Technology
wlli@ntut.edu.tw

ABSTRACT

Nonlinear soft elements are usually effective for vibration reduction. However, most stress-train relations are not exact and have limitation of materials and scale. It's desirable to develop other kinds of nonlinear isolators to improve it. Anticipating the effect of such a system is similar to a soft spring system, one can have a certain extend to design diverse kinds of soft spring terms. Especially, liquid is used to build the isolation systems.

In this paper, three types of nonlinear liquid systems (NLS) are introduced, which are the exchange, buoyance and loading types. They are variable mass systems. The equations of motion of these systems are also derived to verify their nonlinearities. Numerical simulations are followed for several example shapes. The analysis results show soft spring effects. An experimental model is displayed to verify its soft spring effect in the next steps. This paper gives guidelines and suggestions for using NLS as vibration isolators.

Keywords: Liquid system, Nonlinear system, Soft Spring, Variable Mass, Vibration Isolator

1. INTRODUCTION

Passive Isolators or absorbers are adopted to reduce vibrations. No matter the type of the reducing systems, they can be used only in a small frequency range. However, since the existence of nonlinearity in nonlinear systems, the natural frequency can be adjusted, hence it may be more flexible and useful.

In Recent research of nonlinear passive vibration isolators, most of them using soft elements or the balance force curve behave softening so they are effective to reduce the transmissibility of oscillation of systems [1]. For example, Hunt [2] shows a system using a disc spring (cf. Fig. 1) which is a typical soft spring, may have wider suppression band of frequency spectrum.

However, such soft springs usually can not endure large deflection then hard or linear ones, especially during preloading to decrease the natural frequency of the systems [4-7]. On the other hand, most of materials experience their stress-train relations formulas are not very reliable, which are always have limitation of material [4] and sensitive to scales ([6]).

It is desirable that one to consider other ways to develop systems such that they persevere "soft effects." Anticipating the increasing needs for such soft effect isolators from, the present research of attempts to exactly derive and simulate the effects of such nonlinear systems through with fluid ones.

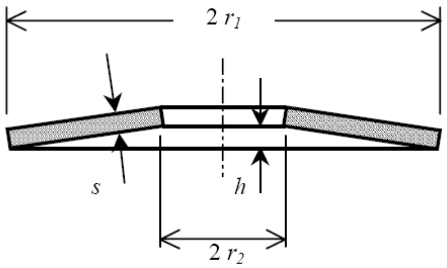

Figure 1. Geometric profile description of a disc spring.

2. Nonlinearity of Vibration Systems

Sources of nonlinearity can be classified to material, geometrical, or associated with nonlinear body forces or physical configuration [8]. In this paper, geometrical and configuration nonlinearity are mainly considered.

In most researches, nonlinearities more often exists in geometrical ways. Systems bring nonlinearity since the special profiles of elements. Generally, they are assumed to be linearly elastic when in small oscillation. However, they obey nonlinear relationships between stress and strain during large deflections. Besides, the stiffness of nonlinear elements may be softening or hardening due to the load-displacement curves.

2.1 Softening elements and their limitation

Gross [3] has shown that the load-displacement relationship of a Belleville spring (or disc spring) made by metal can be written as a function as

$$F(x) = (\frac{Eh^2}{1-\nu^2})(\frac{sx}{nNr_1^2})[(\frac{s}{h})^2 + (1-\frac{x}{Nh})(1-\frac{x}{2Nh})] \quad (1)$$

where E is the Young's modulus,ν the Poisson ratio, N the number of discs, n the dimensionless parameters (detail see [2-4]). Others are geometric parameters (cf. Fig. 1). Eq. (1) can also simply be written to a 3rd-order polynomial function as

$$F(x) = k_1 x + k_2 x^2 + k_3 x^3 \quad (2)$$

Chen [5] further confirmed it by using the disc spring in his frequency-adjustable absorber. However, when Cai [4] changed the material of disc spring to plastics, the load-displacement experiment curve cannot fit the one well by substituting material parameters to eq. (1). It appears even more softening. Hence eq. (1) depends on the diversity of material of disc springs.

Lin [6] and Wang [7] consulted the profiles of disc and wave springs as well as many other soft elements and

created their own soft elements for their isolators. In their results, the stiffness is sensitive to the thickness of the components, and it's hard to give a mathematical formula. They all checked the elements by CAD/CAE and confirmed by tensile tests. However, it costs a lot and sometimes leads to different curves unfortunately.

Virgin [9] used a highly deformed polycarbonate strip clamped together at the end and attached to a vertically oscillating base for an isolation element to reduce the motion of a supported mass. He derived the governing eqns. using an elastica analysis [10]. And he solved numerically the eqns. using a shooting method to satisfy the boundary condition. The numerical results almost fit the experimental ones about force-deflection relationship. Numerical method may be more reliable, but it's too complex to get the right answer.

The present research attempts to find out simpler and exact rules for producing soft spring effects of vibration isolation systems.

2.2. The Soft Spring Effects

Some configuration nonlinear systems give ideas to get the soft effects. Carrella et al. [11] used two oblique springs into their system (Fig. 2). The force-displacement relation about oblique springs can be written as

$$f(x) = 2k_0(h_0 - x)\left(\frac{\sqrt{h_0^{\,2} + a^2}}{\sqrt{(h_0 - x)^2 + a^2}} - 1\right) \qquad (3)$$

which refers to a hardening curve. While they set the combined point with an offset or an initial angle of the oblique spring, it can behave softeningly. Specially, it is quasi-zero stiffness when moving near horizontal line *MN*. It has no argument about the results since the formula can be readily derived by statics. One can have the exact eq. of motion of the system by equation (3) and the constant stiffness of the linear spring. One can also tune the natural frequency of the system like preloading soft elements by set different initial angle or changing different springs of different stiffnesses to get a new force-displacement curve. Chen shows another case. A linear spring passing horizontally through a non-constant cross-section channel (cf. Fig. 3) [12]. The force-displacement relation can be written as

$$F(x) = 4k\int_0^x f'(x)^2 dx \qquad (4)$$

where $f(x)$ is the channel's profile function.

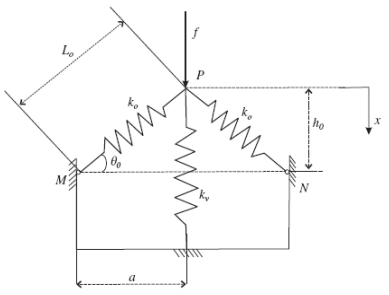

Figure 2. Schema of the oblique spring system. [11]

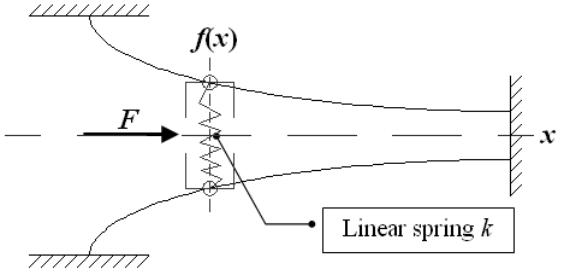

Figure 3. Linear spring moves in a variation channel.

Theoretically, one can substitute any satisfactory function into equation (5) and then get the softening spring term. Therefore, the complete behaviors can be obtained. These two examples show that one can design the spring term in certain range freely by using configuration nonlinearity. The present research even suggests one to extend the results to higher degree of freedom systems.

3. Systems using Liquid

Relatively, few researches consider using liquid to build an isolation system, or just like discussing vibration isolation of liquid storage tanks [1]. The main reason may be hard to describe the motion of liquid exactly, since it's not rigid body. However, it still can have an approximate solution under some assumptions.

Liquid offers mass, damping and probably nonlinearity as well due to the frame of the system. It's interesting to find out what kind of frames can lead to soft effects.

This paper will discuss three types of NLS that producing soft spring effects for vertical vibration isolation by its configuration. Besides, all three types have the similar idea – liquid flow through variation frame.

3.1 The Exchange Type

The word "exchange" here means the liquid can flow between a few manifolds or chambers in the system. A basic example is u-tube manometer (cf. Fig. 4). The whole tube has the same cross-section. For the initial state one side rises x and another size drops the same. It's a linear system and the natural frequency [15] is

$$\omega_n = \left(\frac{2g}{l}\right)^{1/2} \qquad (5)$$

where the notations are shown in the figure.

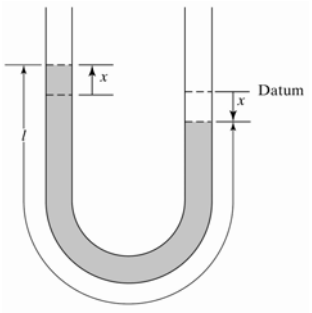

Figure 4. U-tube manometer [15].

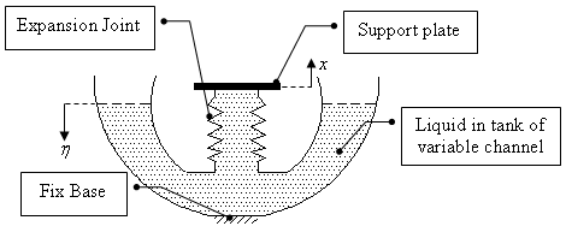

Figure 5. Variation Channel with Expansion Joint.

Deng [13] showed that by different cross-section areas of input and output side like jacks using oil pressure. The vibration may be reduced for the specific ratio of area in certain conditions.

The present research then guesses if the exchange type brings up nonlinearity, it does not depend on the different section of chamber, but at least one side has variation section through the channel.

A Single D.O.F. NLS of exchange type (NLS-E) with variation channel is revealed by improving the model Chen [10] revealed. The sketch is shown in Fig. 5. One neglects sloshing and surface tension of liquid and assumes for the steady flow and the cover of liquid balance instantly. The cover of liquid will flow following the variation channel with η witch can be derived to a one-to-one function of x, which is the displacement of the plate. Since the height of liquid may vary nonlinearly, it will lead to various nonlinear terms that corresponding to the profiles.

3.2 The Buoyance Type

According to Archimedes' principle [14], any object, wholly or partially immersed in a fluid, buoys up by a buoyant force equals to the weight of the fluid that displaced by the object (cf. Fig. 6). Besides, Archimedes' principle does not consider the surface tension (capillarity) acting on the body. The paper also neglects it here. The assumption is the same to what this paper has brought up in exchange type.

A buoyancy system using a dobber attached to a support mass is shown in Fig. 7. The relationship between the displacement x and the volume of the fluid displaced by the dobber can be nonlinear due to the non-constant cross-sectional area of the dobber.

By the conservation of mass, cf. Fig. 7, the equation of motion for undamped free vibration is

$$m\ddot{x} + kx + \rho B(x) = m\ddot{x} + f(x) = 0 \qquad (6)$$

where m is the total mass of dobber and support plate, k the stiffness of the linear spring, and ρ the density of liquid. The buoyancy function can be expressed as

$$B(x) = -\int_0^{L_0-(x+\eta)} A(\xi)d\xi = A_0\eta \qquad (7)$$

where L_0 is the height of the dobber sink into the liquid initially, A_0 the constant section area of the tank, $A(\xi)$ the section profile function (i.e. ξ is not a displacement variable) of the dobber and η the displacement variable of liquid cover. This paper analysis an example with a symbolic section profile as

$$A(\xi) = A_1 + s(\xi - L_0)^2 \qquad (8)$$

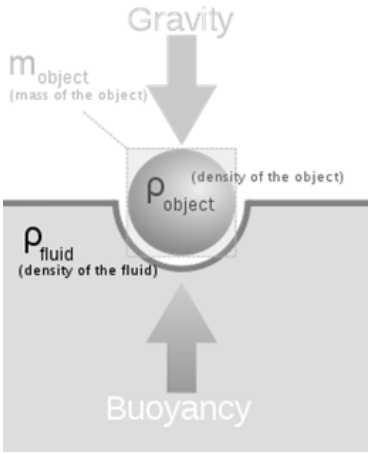

Figure 6. The forces at work in buoyancy [14]

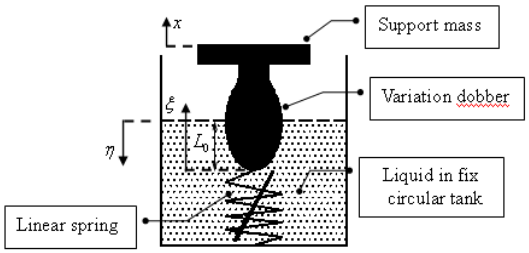

Figure 7. The forces at work in buoyancy.

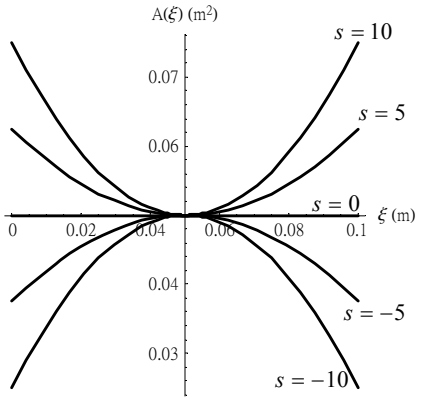

Figure 8. Plot of eq. (8) for $A_1 = 0.05\text{m}^2$ and $L_0 = 0.05\text{m}$ with different coefficient s.

which is a symmetric shape. A_1 is the section area of dobber at static surface. A sample plot of $A(\xi)$ with different coefficient s is shown in Fig. 8 (S.I. unit).

If A_0 is much greater than the maximum of $A(\xi)$, which means the tank is extreme large, one can easily integrates equation (8) by letting $\eta = 0$. However, this paper considers the existence of η.

Refer to Fig. 8, if s is positive, the cross-section of the dobber gets wider from $\xi = L_0$ to both sides and for negative s it gets narrower. The present research believes the soft spring effects will occur for either wider or narrower case.

In order to get a desired nonlinear element, the present research suggests that the two steps: (1) To determine the profile function of the cross sectional area; and (2) To derive a one-to-one function of x by using eq. (7) to obtain parameter η. By substituting equation (8) to

eq. (7), one yields

$$(x+\eta)[A_1+\frac{s}{3}(x+\eta)^2]-A_0\eta=0 \qquad (9)$$

which is obvious an implicit function of x. The plot that using the same parameters as in Fig. 8 is shown in Fig. 9. Notice that the direction of variable x and η must be the same sign. One can only consider the curve in the first and third quadrant. Besides, the dobber is limited not to leave the liquid. In other words, it leads the limitation function to $\eta + x = L_0$. In addition, one considers the dobber always touches the liquid, it thus leads to another limitation function: $\eta + x = -L_0$. As a consequence, the available moving range locates in the triangle regions in the first and the third quadrant, shown in Fig. 9.

For an approximate solution of the curve, one is to consider small oscillations of the plate. In the mean time, the cubic terms of x and η in eq. (9) are neglected. For a simple comparison, one considers the case $s = \pm 10$, shown in Fig. 8. As s = -10, $A_0 = 0.1\text{m}^2$, $A_1 = 0.05\text{m}^2$ and L_0 = 0.05m, one solves equation (9) and yields

$$\eta^*(x)=\frac{(-0.05^2-0.5x^2+0.5\sqrt{x^4+0.03x^2+0.005^2})}{x} \qquad (10)$$

It's convenient to use the Taylor expansion of eq. (10) to have a polynomial function. Keeping up to the cubic terms, one yields

$$\eta_T(x)=x-400x^3 \qquad (11)$$

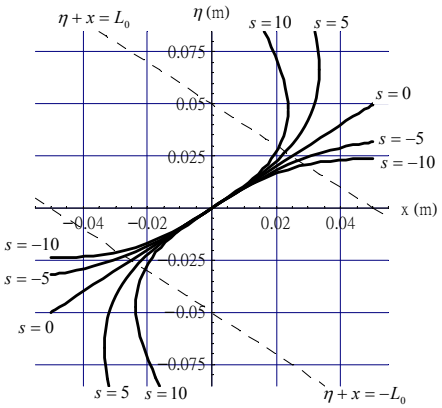

Figure 9. Plot of eq. (9)

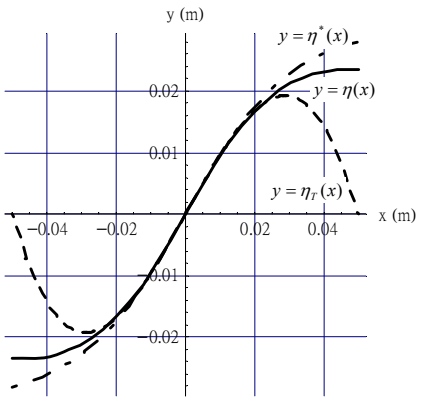

Figure 10. Comparison plot of case s = -10.

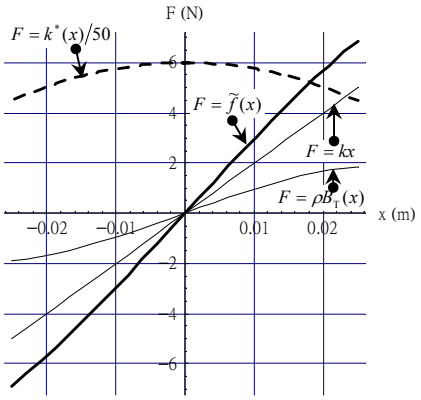

Figure 11. Force combination curve of case s = -10 For k = 200 (N/m), ρ= 1000 (kg/m^3).

The comparison plot is shown in Fig. 10. eq. (11) shows well approximation for $|x|$ less than about 0.02. One can just substitute eq. (11) to eq. (7) and get the approximate buoyancy variation function, which is

$$B_T(x)=A_0\eta_T(x)=0.1x-40x^3 \qquad (12)$$

Fig. 11 shows the force combination curve for the specified values, where the approximate spring term of eq. (6) is determined as

$$f(x)\cong\tilde{f}(x)=kx+\rho B_T(x)=300x-40000x^3 \qquad (13)$$

in which the stiffness function is

$$k^*(x)=\frac{\partial f(x)}{\partial x}=300(1-400x^2) \qquad (14)$$

In this case, eq. (14) is valid for $|x|$ less than ca. 0.02. Notice also that the negative stiffness function s shows a softening result which is what one is looking for.

For another case s = 10, using the same parameters as those in Fig.8 and deriving the relative functions, one obtains the followings:

$$\eta^*(x)=\frac{(-0.05^2-0.5x^2+0.5\sqrt{x^4-0.03x^2+0.005^2})}{x} \qquad (15)$$

$$\eta_T(x)=x+400x^3 \qquad (16)$$

$$B_T(x)=A_1\eta_T(x)=0.1x+40x^3 \qquad (17)$$

$$f(x)\cong\tilde{f}(x)=kx+\rho B_T(x)=300x+40000x^3 \qquad (18)$$

$$k^*(x)=\frac{\partial f(x)}{\partial x}=300(1+400)x^2 \qquad (19)$$

Plots are shown in Figs. 12 and 13. Notice that the stiffness function shows a hardening result. Thus, the soft effect of NLS of the buoyance type (NLS-B) occurs only as s is negative. The works above are done with the help of Mathematica [17].

Specially, one further considers the case s = 0, with the diameter of the dobber d_0 and the diameter of the tank D_0. Solving eq. (8) and substituting into eq. (7), one has

$$m\ddot{x}+[k+\rho\frac{\pi D_0^{\,2}d_0^{\,2}}{4(D_0^{\,2}-d_0^{\,2})}]x=0 \qquad (20)$$

which shows a linear equation as one expect.

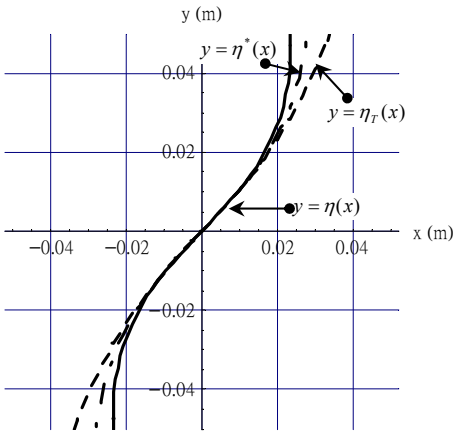

Figure 12. Comparison plot of case s = 10.

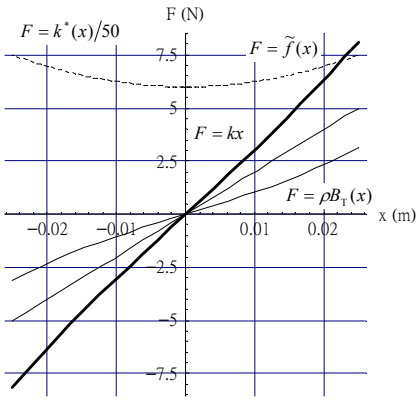

Figure 13. Force combination curve of case s = 10 for k = 200 (N/m), ρ= 1000 (kg/m^3).

It's rational to guess that if this NLS-B perseveres soft spring effects, the cross-section area of the dobber should get narrower from the static surface. Theoretically, one can design a soft spring term whatever one wants by using eq. (7). If one neglects the spring (i.e. k = 0), the rule of the dobber shape still keeps the same. However, one may need to take the limit of the maximum loading into account.

4.3 Loading Type

Considering a similar idea, the loading type (NLS-L) further uses the mass of liquid, and the system can behave a variable mass term. In fact, a typical system was introduced by Singiresu [15] and Hartog [16] shown in Fig. 14. The system contains two circular tanks, a plate slides in one of the tanks, a linear spring for supporting the plate, and some kind of liquid storage in the tank. The instant loading of the system (dashed rectangle) depends on the displacement x, and so nonlinearity may appear in the mass term. The present research generalizes the system to a variation profile. But the first important work is to discuss whether the specific diameter ratio of the original system may lead to soft effect or not.

The demonstration structure is shown in Fig. 15. A transfer region is added into the original system for flowing smoothly of the liquid. The assumption is the the same as the case of NLS-B. To derive the equation of motion, one uses the Lagrange Equation. Or, the kinetic energy can be written as

$$T=\frac{1}{2}[m_0+\rho A_0(L_0-x)+\rho A_0\alpha^2(L_1+\alpha^2 x)+\rho A_0^{\,2}\int_0^L\frac{d\xi}{A(\xi)}]\dot{x}^2 \tag{22}$$

where ρ is the density of liquid, α the diameter ratio. And α satisfies $\alpha^2 = A_0/A_1$, which is area ratio.

Assume the bases are all fixed (i.e. $u(t)$ = 0), the potential energy can be written as

$$V=\frac{1}{2}[k+\rho A_0 g(1-\alpha^2)]x^2 \tag{23}$$

where g is gravity acceleration. By the principle of conservation of mass, one can easily derive the displacement variable $\eta(x) = \alpha x^2$. By substituting it into the process for deriving kinetic and potential energy, the variable is vanished and the system becomes single D.O.F. system.

The Lagrange equation can be written as

$$\frac{d}{dt}\left(\frac{\partial T}{\partial \dot{x}}\right)-\left(\frac{\partial T}{\partial x}\right)+\left(\frac{\partial V}{\partial x}\right)=F(t) \tag{24}$$

Consider the transfer region of the system with the function $A(\xi) = A_0+(A_1-A_0)(\xi/L)^2$, by substituting it and eq. (22), eq. (23) into eq. (24), yields

$$[m_0+\rho A_0(L_0+\alpha^2 L_1+\alpha L)]\ddot{x}+[k-(1-\alpha^2)\rho A_0 g]x+\rho A_0(\alpha^4-1)[0.5\dot{x}^2+x\ddot{x}]=F(t) \tag{25}$$

which is the eq. of motion.

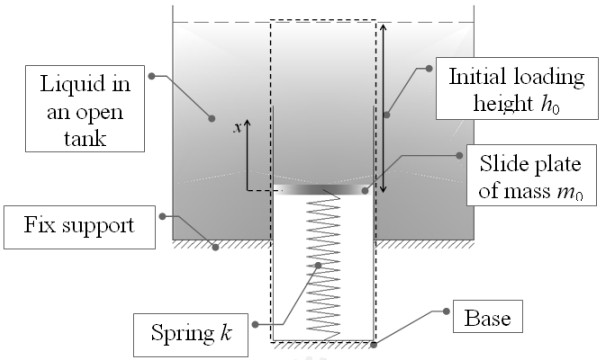

Figure 14. Variable mass system [13]

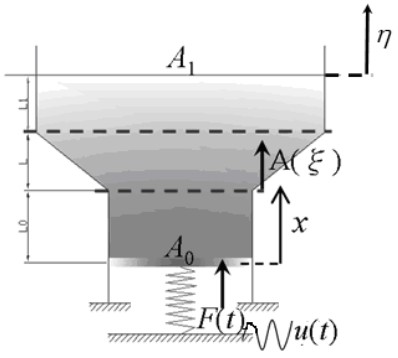

Figure 15. Different diameter tanks with transfer region.

The nonlinear term appears at the LHS is from the nonlinear momentum. The straight velocity profiles are different for the two section areas. And, the mass variable and the loading vary with the variable x.

A standard form with viscous damping is then

$$\ddot{x} + 2\zeta\omega_0\dot{x} + \omega_0^2 x + \gamma\omega_0^2(0.5\dot{x}^2 + x\ddot{x}) = f(t) \qquad (26)$$

where the natural frequency is

$$\omega_0 = \sqrt{g(P_k + \alpha^2 - 1)/[L^*(P_m + 1)]} \qquad (27)$$

with the nondimensional parameters

$$P_k = \frac{k}{\rho A_0 g}, P_m = \frac{m0}{\rho A_0 L^*} \qquad (28)$$

The equivalent length in eq. (28) is defined as

$$L^* = L_0 + \alpha^2 L_1 + \alpha L \qquad (29)$$

and the nonlinear factor is

$$\gamma = g^{-1}\frac{\alpha^4 - 1}{P_k + \alpha^2 - 1} \qquad (30)$$

Though the numerator of eq. (27) may be negative or positive, for stability of the system requires the natural frequency to be a positive real number, hence $P_k + \alpha^2 > 1$ and the sign of γ is due the diameter ratio α (or area ratio α^2). A contour plot is shown in Fig. 16 for an example. Notice that the region is only valid in $P_k + \alpha^2 > 1$ (i.e. the right upper side above the oblique line $P_k + \alpha^2 = 1$). Besides, γ is negative over the left side ($\alpha < 1$) of the straight line $\alpha = 1$ and positive over the right side $\alpha > 1$.

The system (26) is applied by a swept-sine analysis to verify whether the natural frequency will shift with the nonlinear factor or not. The SIMULINK [18] model is shown in Fig. 17.

For reason of demonstration, one sets the frequency range of a chirp signal from 0 to $4\omega_0$ in 20 sec as same as sampling time (i.e. the precision of response spectrum is 0.05 Hz) and the sampling frequency to $10\omega_0$ since it's enough. Fix-step solver ode3 (Bogacki-Shampine method).

The spectrum of the Chirp signal is shown in Fig. 18, and a typical output spectrum with nonlinear factor is shown in Fig. 19. The Plot of the magnification factor to the nonlinear factor is shown in Fig. 20 and Table 2.

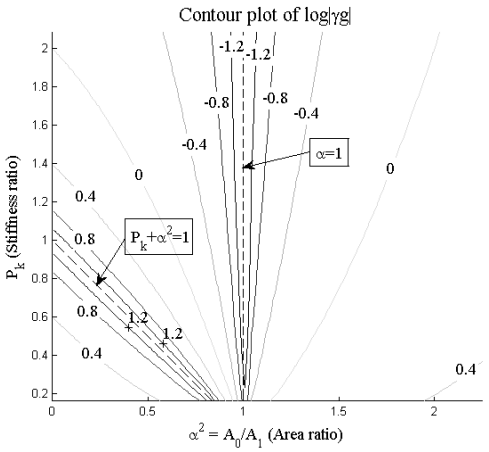

Figure 16. Contour Plot about eq. (30).

Analysis results show that for the larger magnitude of nonlinear factor, the less magnification factor. It's mainly due to the last nonlinear term in eq. (26).

However, on the other hand, the max response frequency is still kept the same as the original natural one. In fact, this phenomenon holds for other original natural frequencies or magnitudes when applying chirp signals A_m. The reason can be refer to the static status, i.e. $\dot{x} = \ddot{x} = 0$, since the linear relationship between the balance force and the displacement x.

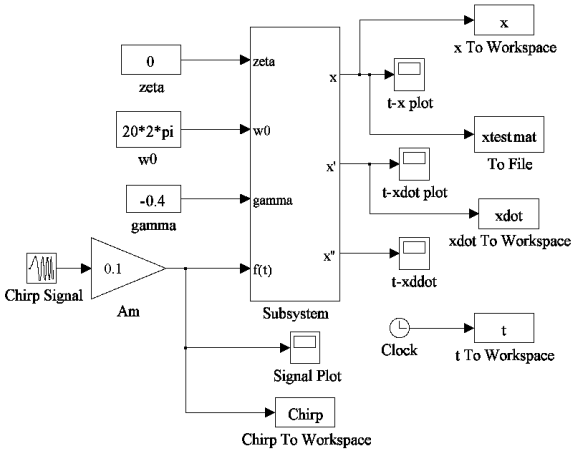

Figure 17. Simulink model of eq. (26).

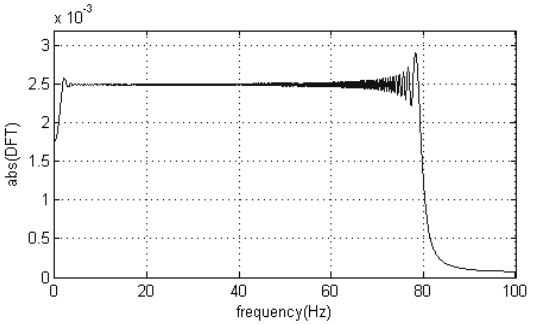

Figure 18. Frequency spectrum of Chirp Signal.

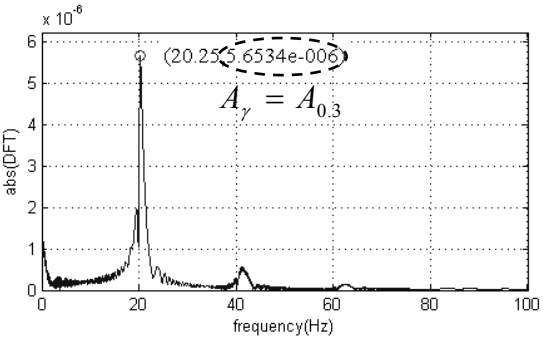

Figure 19. Outputs spectrum for parameters $\omega_0 = 40\pi$, $\zeta = 0$, $\gamma = 0.3(\alpha>1)$, $A_m = 0.1$

Table 2. Magnification factor $M_\gamma = A_\gamma\omega_0^2/A_m$

γ	-0.3	-0.2	-0.1	0	0.1	0.2	0.3
M_γ	0.860	1.255	1.369	1.401	1.376	1.269	0.893
$\frac{M_\gamma}{M_0}$	61.36 %	89.58 %	97.71 %	100 %	98.2 %	90.55 %	63.71 %

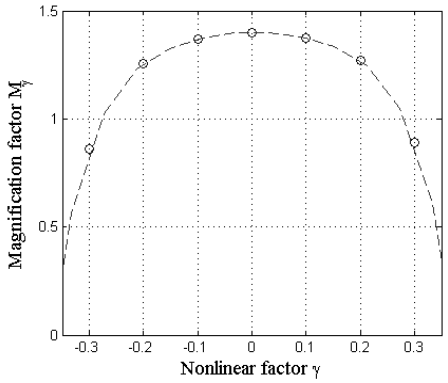

Figure 20. Plot of Magnification to nonlinear factor.

Although the amplitudes of the vibration do not reduce obviously as the nonlinear factor varies, the non-constant section profiles do keep the characteristics of soft springs. Fig. 21 shows a general structure. It's unnecessary to make a variation section container, but use a cylinder tank with a variation section core to achieve the variation section frame. The kinetic energy of such a system can be written as

$$T = \frac{1}{2}[m_0\dot{x}^2 + \rho A_0(L_0 - x)\dot{x}^2 + \rho {A_0}^2 \dot{x}^2 \int_0^{L_1+\eta} \frac{d\xi}{A(\xi)}] \quad (31)$$

Notice that the upper limitation of integration is a constant in eq. (22) while a function of x in equation (31). Assume the base is fixed (i.e. $u(t) = 0$), the potential energy can be written as

$$V = \frac{1}{2}[k - A_0\rho g]x^2 + \rho g \int_{L_1}^{L_1+\eta} A(\xi)(\xi - L_1)d\xi \quad (32)$$

which is more complex than eq. (23), and may lead to a nonlinear spring term since the last term of it.

Eq. (31) and eq. (32) shows the general form of energy for the general NLS-L. The first work is also to derive the displacement of liquid cover $\eta(x)$. According to the principle of conservation of mass yields

$$\int_{L_1}^{L_1+\eta} A(\xi)d\xi = A_0 x \quad (33)$$

For any section profile function $A(\xi)$, the equation of motion can be determined by Lagrange Equation (cf. equation (24)). The eq. of motion with damping force can be written in a general form

$$\ddot{x} + 2\zeta\omega_0\dot{x} + {\omega_0}^2[f(x) + g(x)\dot{x}^2 + h(x)\ddot{x}] = f(t) \quad (34)$$

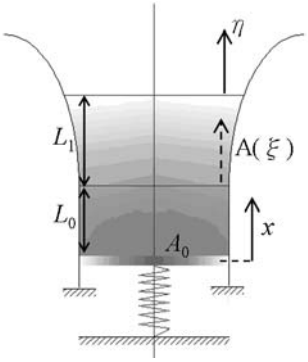

Figure 21. Demonstration of a general structure.

To solve whole term of eq. (34) is not necessary for confirming the soft spring effects. Consider the system is in static status (i.e. $\dot{x} = \ddot{x} = 0$), the relationship between balance force and displacement x is only due to the third term of eq. (32). The present research believes that the soft effect is obtained by the third term of eq. (32), and the last term of eq. (32) reduces the vibration of the system. An experimental structure in introduced in Fig. 22, which is used to verify the LVS-L in the future.

A non-constant cross-section core is put inside the tube instead of making a variation profile tank. External Force from a shaker acts through the rods to slide plate (cf. eq. (32)). One can also considers the base as the machine, and the slide plate as an absorber. Thus the force acts on the base (i.e. $u(t) \neq 0$), yields the equation

$$\ddot{x} + 2\zeta\omega_0\dot{x} + {\omega_0}^2[f(x) + g(x)\dot{x}^2 + h(x)\ddot{x}] = {\omega_0}^2 u(t) \quad (35)$$

By the reference of NLS-B, the cores as modules are considered to make the section area vary from narrow to wide for soft spring effects. Some examples of core are shown in Fig. 23. Specially, type (a) will be used to verify the area ratio effect this paper discussed.

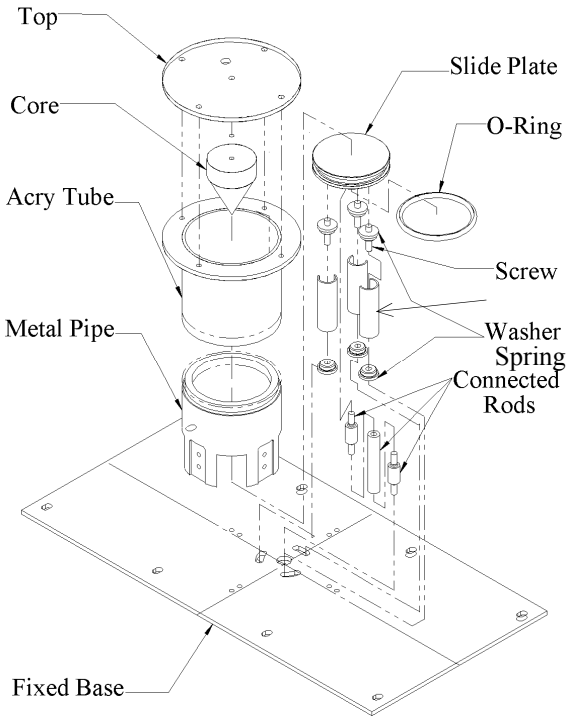

Figure 22. Demonstration of the NLS-L.

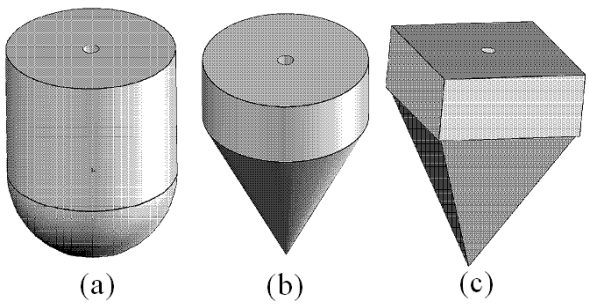

Figure 23. Cores of NLS-L. (a) Cylinder with diversion head (b) Cone (c) Square based pyramid

5. Conclusion

Three types of NLS are discussed in this paper, which consider use liquid in the system and anticipating improving the disadvantages of geometric soft elements. NLS-E first reveals that liquid flow through a variation frame or between different size regions may lead to nonlinearity. NLS-B reduces the natural frequency of the system with the buoyancy, and persevere soft spring effects due to the variation dobber. NLS-L discusses the effects about area ratio of input and output region, and further suggests a general form.

Significantly, an experimental structure is introduced to verify the theory in next steps. It uses non-constant cross-section cores instead of making non-constant cross-section tanks. The present research makes some ideal assumptions of liquid, which may be different in real system in certain conditions.

Specially, these systems show methods to design the shapes of the NLS frame to get softening system. Once the profiles (e.g. dobbers of NLS-B, cores of NLS-L) are decided, the equation of motion as well as the nonlinear effects (usually designs to softening) is determined.

6. REFERENCES

[1] R. A. Ibrahim, "Recent Advanced in nonlinear passive vibration isolators," *Journal of sound and vibration, 314, 2008, pp.371-452*.

[2] J. B. Hunt and J. C. Nissen, "The Broadband Dynamic Vibration Absorber," *Journal of sound and vibration, vol. 83(4), 1982, pp.573-578*.

[3] S.GROSS 1996 *Calculation and Design of Metal Springs*. London: Chapman & Hall Limited.

[4] 蔡忠瑾，應用非線性元件模組之創新微振避振平台研發，國立台北科技大學機電整合研究所，2006.

[5] 陳信宏，頻率可調式非線性微吸振器之研究，國立台北科技大學製造科技研究所，2003.

[6] 林逸倫，非線性元件於隔振之效應分析及驗究，國立台北科技大學製造科技研究所，2008.

[7] 王信富，應用非線性元件於高架地板之創新設計隔振器研究，國立台北科技大學機電整合研究所，2008.

[8] Jon J. Thomsen, "*Vibrations and Stability* (2nd ed.)"

[9] L.N. Virgin, S.T. Santillan, R.H. Plaut, Vibration isolation using extreme geometric nonlinearity, *Journal of Sound and Vibration 315 (2008) 721-731*.

[10] S. Santillan, L.N. Virgin, R.H. Plaut, Equilibria and vibration of a heavy pinced loop, *Journal of Sound and Vibration 288 (2005) 81-90*.

[11] A. Carrella, at el., "Static analysis of a passive vibration isolator with quasi-zero-stiffness characteristic," Journal of Sound and Vibration (2006)

[12] 陳予恕，非線性振動

[13] 鄧錦坤，應用液體體積轉換於導引懸吊系統的結構設計與性能分析，2008.

[14] Wikipedia, "http://en.wikipedia.org/wiki/Buoyancy"

[15] Singiresu S. Rao, "*Mechanical Vibrations* (4th ed.)"

[16] J. P. Den Hartog, "*Mechanical Vibrations* (Dover ed.)"

[17] Mathematica, "http://www.wolfram.com"

[18] Matlab/Simulink, "http://www.mathworks.com"

非線性流體系統於隔振之分析與應用

黎文龍[1]、魏聿彥[2]
[1]教授, [2]學生
國立臺北科技大學
wlli@ntut.edu.tw

摘要

使用一些非線性軟性元件對於振動抑制是有效的。然而，大多數的應力應變經驗公式並不精確且有著材料以及尺寸上的侷限。因此值得發展他種的非線性隔振器來改善。

吾人希望該系統效應類似於使用一軟彈簧之系統，而進一步在一定程度上可自由地設計各式各樣的軟彈簧項次。特別地是，流體將用於構成此隔振系統。

在本報告中介紹了三種型態的非線性流體系統(NLS)，分別是交換型、浮力型以及承載型，他們可能為變動質量系統。本研究也推導了這些系統運動方程式於。在特定造型下，分析結果顯示其具有軟效應。本文展示了一種承載型的實驗架構以供未來驗證其軟效應。總而言之，本文對使用非線性流體系統作為隔振器提出一些指引與建議。

關鍵詞：流體、非線性、軟彈簧、變動質量、隔振器